Bioactive Rearranged and Halogenated Semisynthetic Derivatives of the Marine Natural Product Sarcophine

Swapnali S. Sawant,[†] Paul W. Sylvester,[†] Mitchell A. Avery,[‡] Prashant Desai,[‡] Diaa T. A. Youssef,[§] and Khalid A. El Sayed*[,†]

Department of Basic Pharmaceutical Sciences, School of Pharmacy, University of Louisiana at Monroe, 700 University Avenue, Monroe, Louisiana 71209, Department of Medicinal Chemistry, School of Pharmacy, The University of Mississippi, University, Mississippi 38677, and Department of Pharmacognosy, Faculty of Pharmacy, Suez Canal University, Ismailia 41522, Egypt

Received August 6, 2004

Cembranoids are natural diterpenes with 14-membered macrocyclic rings. The simplest natural cembranoid, (+)-cembrene, was isolated from pine oleoresin. Sarcophytols A and B are known cembranoids that inhibit tumor promotion. Sarcophine is a related cembranoid isolated from the Red Sea soft coral *Sarcophyton glaucum*. Sarcophine and its bioconversion products and semisynthetic derivatives are reported to possess cancer chemopreventive activity. Oxymercuration−demercuration of sarcophine using $Hg(OAc)_2$ and $NaBH_4$ afforded four new rearranged and hydroxylated products. Bromination of sarcophine with *N*-bromosuccinimide (NBS) furnished two new brominated and rearranged products. Reaction with iodine gave the known iso-sarcophinone and (+)-sarcophytoxin B. Structure elucidation was based on a combination of transition state modeling, molecular dynamics, mechanistic considerations, and 2D NMR data. The antiproliferative activity of the new products is also reported.

In 1962, the first cembranoid diterpene, (+)-cembrene (**1**), was reported from pine oleoresin.[1,2] This was followed by the isolation of hundreds of cembranoids from plants and insects as well as of marine origin.[3] These compounds are known to be the main chemical defense tools of the marine soft corals against their natural predators. Cembranoids either are feeding deterrents or act by virtue of their toxicity.[4] Sarcophytols A (**2**) and B (**3**) are important cembranoids that show cancer chemopreventive activity.[4,5] Sarcophytol A inhibits tumorigenesis with a wide array of mechanisms.[5] Sarcophine (**4**), a related cembranoid, was first reported by Kashman and co-workers in 1974 from the Red Sea soft coral *Sarcophyton glaucum*.[6] It was shown to have a diverse biological activity range.[7−10] Sarcophine is structurally related to **2**, and its availability (up to 3% dry weight) further encouraged additional chemical and pharmacological studies. Earlier attempts involved both microbial and semisynthetic transformation of sarcophine to generate new derivatives with chemopreventive activity.[10,11] Both studies revealed that the hydroxylated derivatives improved the anticancer activity. This prompted the investigation of oxymercuration of sarcophine using mercuric acetate and sodium borohydride, which would lead to the hydroxylated rearranged products. This reaction type, in which a mercuronium ion is opened by an intervening epoxide, has been reported in the formation of a monocyclic ring system from the acyclic epoxy-olefin, α,β-epoxyartemisia ketone.[12] It is an underexplored and potentially useful reaction for formation of ether-bridged macrocyclic natural products.[13] Also, iodination of sarcophine-related cembranoids has been shown to enhance their bioactivities, and hence halogenation of sarcophine was attempted.[14]

Results and Discussion

Oxymercuration of sarcophine (**4**) yielded compounds **5**−**8** in 57.8% combined yield. The HRFABMS spectrum of **5** displayed a molecular ion peak at *m/z* 353.2328 $[M + H]^+$, suggesting the molecular formula $C_{20}H_{32}O_5$ and five degrees of unsaturation. The IR absorption band at 1183 cm^{-1} suggested the presence of an ether bridge. The ^1H and ^{13}C NMR data of **5** (Table 1) further corroborated this assignment. The ^1H NMR spectrum of **5** shows only one downfield signal at δ 5.13. On the basis of its ^3J-HMBC correlation with C-15 (δ 123.6) and ^2J-HMBC correlation with C-1 (δ 163.9) this proton was assigned as H-2. The absence of other olefinic ^1H signals suggested that addition to both $\Delta^{3,4}$ and $\Delta^{11,12}$ olefins had occcurred. The quaternary carbon at δ 82.1 was assigned as C-4 on the basis of its ^3J-HMBC correlation with H-2. C-4 also showed a ^2J-HMBC correlation with the methyl singlet H_3-18 (δ 1.44). ^1H and ^{13}C NMR data of **5** also revealed the absence of the C-7/C-8 epoxide functionality. The downfield proton at δ 4.00 (δ_C 88.7) was assigned as H-7 on the basis of its ^3J-HMBC correlation with the methyl singlet C-19 (δ 25.0) and ^2J-HMBC correlation with the C-6 (δ 20.5) and the quaternary oxygenated C-8 (δ 73.4). These data suggest the ether bridge to be positioned between C-4 and C-7. These assignments perfectly match with the previously reported ^{13}C chemical shifts of ether-bridged cembranoids.[15,16] The ^1H NMR showed that all of the methyl signals were singlets, indicating that the remaining C-20 methyl must be located on the quaternary C-12 carbon. The quaternary oxygenated carbon placed at δ 73.2 was assigned as C-12 on the basis of its HMBC correlation with H_3-20.

The HRFABMS data of **6** suggested that it is an isomer of **5**. The quaternary carbon at δ 73.3 was assigned to C-4 on the basis of its ^3J-HMBC correlation with H-2. The upfield shift of C-4 in **6**, compared with that in **5**, suggested that C-4 in **6** is bearing a free hydroxy group instead of an ether oxygen. The proton doublet of doublets resonating at δ 3.04 is assigned to H-7 on the basis of its HMBC correlations with C-8 (δ 69.9) and C-19 (δ 20.7). The methyl doublet at δ 0.79 was then assigned to H_3-20. This methyl doublet shows ^3J-HMBC correlation with the oxygenated methine carbon at δ 83.9 (C-11) and ^2J-HMBC correlation with the methine carbon at δ 33.1 (C-12).

* To whom correspondence should be addressed. Tel: 318-342-1725. Fax: 318-342-1737. E-mail: elsayed@ulm.edu.
[†] University of Louisiana at Monroe.
[‡] University of Mississippi.
[§] Suez Canal University.

10.1021/np0497393 CCC: $27.50
Published on Web 11/25/2004

Table 1. ^{13}C and ^{1}H NMR Data of Compounds **5**−**7**[a]

	5		**6**		**7**	
position	δ_C	δ_H	δ_C	δ_H	δ_C	δ_H
1	163.9, qC		165.7, qC		164.6, qC	
2	78.5, CH	5.13, brd (8.4)	81.9, CH	5.49, d (9.2)	80.1, CH	5.43, dq (9.9,1.8)
3	44.7, CH_2	2.05,m 1.38, dd (15.0, 8.4)	40.2, CH_2	2.25, d (15.0), 1.15, m	119.3, CH	5.04, d (9.9)
4	82.1, qC		73.3, qC		144.2, qC	
5	40.1, CH_2	2.11, m 1.94, m	39.9, CH_2	1.55, 2H, m	37.3, CH_2	1.98, m 1.94, m
6	20.5, CH_2	1.65, m, 1.36, m	22.7, CH_2	1.79, m 1.62, m	20.0, CH_2	1.56, m 1.27, m
7	88.7, CH	4.00, dd (11.3, 4.8)	85.7, CH	3.04, dd (11.7, 2.2)	84.9, CH	3.06, dd (9.5, 1.4)
8	73.4, qC		69.9, qC		69.9, qC	
9	36.0, CH_2	1.68, 2H, m	34.3, CH_2	1.91, 2H, m	40.2, CH_2	2.54, 2H, ddd (12.8, 12.4, 6.3)
10	19.3, CH_2	1.21, m 1.18, m	31.1, CH_2	1.94, m 1.52, m	27.6, CH_2	2.15, m 1.49, m
11	38.3, CH_2	1.84, 2H, m	83.9, CH	3.39, m	82.3, CH	2.95, 2H, ddd (10.8, 9.9, 2.0)
12	73.2, qC		33.1, CH	1.82, m	38.0, CH	1.25, m
13	39.2, CH_2	1.55, m 1.40, m	23.3, CH_2	2.45, m 1.16, m	31.0, CH_2	1.92, 2H, m
14	26.1, CH_2	2.73, ddd (13.2, 10.6, 8.8) 2.10, m	24.2, CH_2	2.71, ddd (13.2, 13.0, 4.0) 2.44, m	24.7, CH_2	2.46, m 2.43, m
15	123.6, qC		124.0, qC		122.3, qC	
16	174.5, qC		174.7, qC		174.2, qC	
17	8.5, CH_3	1.80, 3H, brs	8.6, CH_3	1.81, 3H, brs	8.8, CH_3	1.82, 3H, brs
18	28.2, CH_3	1.44, 3H, s	28.9, CH_3	1.17, 3H, s	19.3, CH_3	1.85, 3H, s
19	25.0, CH_3	1.07, 3H, s	20.7, CH_3	1.19, 3H, s	20.0, CH_3	1.15, 3H, s
20	30.0, CH_3	1.24, 3H, s	19.0, CH_3	0.79, 3H, d (7.0)	17.2, CH_3	0.88, 3H, d (6.9)

[a] In $CDCl_3$, 400 MHz for ^{1}H and 100 MHz for ^{13}C NMR. Coupling constants (J) are in Hz.

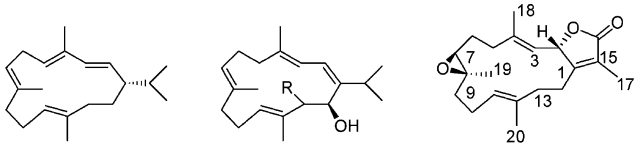

1

2 R= H
3 R= β-OH

4

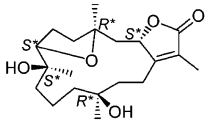

5

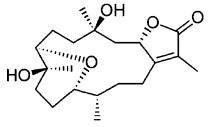

6

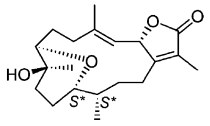

7

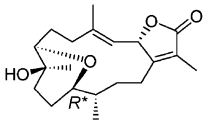

8

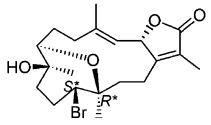

9

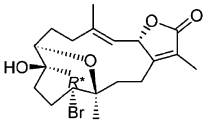

10

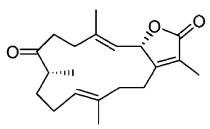

11

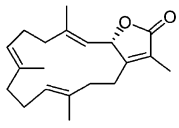

12

The HRFABMS spectrum of **7** suggested the molecular formula $C_{20}H_{30}O_4$ and six degrees of unsaturation. The ^{1}H and ^{13}C NMR data (Table 1) suggest the presence of one double bond in the macrocycle. The most downfield signal at δ 5.43 was assigned to H-2. The COSY coupling of H-2 with the olefinic proton doublet at δ 5.04 indicated the presence of a $\Delta^{3,4}$ system. This was also confirmed by ^{3}J-HMBC correlation of H-2 with C-4 (δ 144.2) and ^{2}J-HMBC correlation with C-3 (δ 119.0). The rest of the molecule was similar to **6**, with the ether bridge between C-7 (δ 84.9) and C-11 (δ 82.3).

The HRFABMS spectrum of **8** displayed a molecular ion peak at *m/z* 335.2213 $[M + H]^+$, suggesting the molecular formula $C_{20}H_{30}O_4$ and six degrees of unsaturation. The similarity of the NMR data of **8** (Table 2) and **7** (Table 1) suggests that they are epimers. The significant difference in the chemical shift and J values of H-11 (δ 3.37, dd, 8.8, 2.2 Hz) in **8** compared to those of H-11 (δ 2.95, ddd, 10.8, 9.9, 2.0 Hz) in **7** indicated that **8** is the C-11 epimer of **7**. This is further supported by a 4.5 ppm difference in the ^{13}C chemical shift value of C-11 between **7** and **8**.

Reaction of **4** with NBS in aqueous acetone at room temperature yielded **9** and **10** in a 22% overall yield. The HRFABMS spectrum of **9** displayed a molecular ion peak at *m/z* 413.1327 $[M + H]^+$, suggesting the molecular formula $C_{20}H_{29}BrO_4$ and six degrees of unsaturation. Compound **9** shows IR absorption bands at 1257 and 1028 cm^{-1}, suggesting the presence of an ether bridge and C−Br linkage, respectively. The ^{1}H and ^{13}C NMR data (Table 2) suggest the presence of a macrocyclic double bond. The $\Delta^{3,4}$ system and epoxide ring opening were confirmed in the same way for **7**. All methyl signals were singlets, indicating substitution at C-12. The quaternary carbon C-12 was assigned at δ 80.0 on the basis of its ^{3}J-HMBC correlation with H-10a (δ 1.99, m) and ^{2}J-HMBC correlation with the methyl singlet H_3-20 (δ 1.69). The methyl H_3-20 also shows ^{3}J-HMBC correlation with C-11 (δ 68.2). The proton H-11 shows COSY coupling with H-10, which further helped to confirm the assignment of C-11.

The HRFTMS spectrum of **10** suggested the same molecular formula as for **9**. The NMR data of **10** (Table 2) indicated an epimeric relationship between compounds **9** and **10**. This was based on the large differences in the proton and carbon chemical shifts at C-11 in **9** and **10**.

Reaction of **4** with I_2/Ph_3P in CH_2Cl_2 in an ice bath for 6 h afforded iso-sarcophinone (**11**) and (+)-sarcophytoxin B (**12**) in 69% overall yield. Neither compound displayed any

Table 2. ^{13}C and ^{1}H NMR Data of Compounds **8**−**10**[a]

	8		**9**		**10**	
position	δ_C	δ_H	δ_C	δ_H	δ_C	δ_H
1	163.9, qC		162.5, qC		163.2, qC	
2	79.9, CH	5.38, dq (10.2, 1.8)	80.1, CH	5.34, dq (9.9, 1.8)	80.3, CH	5.43, d (10.6)
3	119.3, CH	5.11, d (10.2)	118.8, CH	5.09, dq (10.2, 1.1)	121.0, CH	5.14, dq (11.0, 1.1)
4	143.5, qC		146.0, qC		147.8, qC	
5	36.2, CH_2	2.35, m 2.30, m	36.5, CH_2	2.32, m 2.22, m	35.6, CH_2	1.88, m
6	20.5, CH_2	1.58, m 1.46, m	24.8, CH_2	1.95, m 1.61, m	30.0, CH_2	2.17, m 1.45, m
7	83.7, CH	3.03, dd (10.2, 2.9)	84.1, CH	3.08, dd (9.5, 2.9)	77.4, CH	3.14, d (4.4)
8	70.2, qC		70.0, qC		69.1, qC	
9	41.0, CH_2	2.25, m 1.84, m	40.5, CH_2	2.11, m	45.6, CH_2	1.80, m
10	27.6, CH_2	1.64, m 1.37, m	24.7, CH_2	1.99, m 1.57, m	24.5, CH_2	2.05, m
11	77.8, CH	3.37, dd (8.8, 2.2)	68.2, CH	3.58, m	59.1, CH	3.94, d (10.2)
12	36.0, CH	1.51, m	80.0, qC		79.0, qC	
13	31.4, CH_2	1.92, m 1.84, m	39.6, CH_2	1.32, m 1.05, m	31.1, CH_2	1.78, m
14	23.0, CH_2	2.33, m 2.05, m	22.8, CH_2	2.68, ddd (12.7, 11.6, 7.0) 2.00, m	24.2, CH_2	2.50, m 2.45, m
15	122.9, qC		124.5, qC		123.8, qC	
16	176.1, qC		175.5, qC		174.1, qC	
17	8.8, CH_3	1.83, 3H, brs	9.1, CH_3	1.80, 3H, brs	8.9, CH_3	1.83, 3H, brs
18	16.4, CH_3	1.82, 3H, s	17.8, CH_3	1.86, 3H, s	22.9, CH_3	2.04, 3H, s
19	20.5, CH_3	1.16, 3H, s	20.3, CH_3	1.15, 3H, s	20.8, CH_3	1.17, 3H, s
20	14.6, CH_3	0.87, 3H, s	27.4, CH_3	1.69, 3H, s	22.0, CH_3	1.25, 3H, s

[a] In $CDCl_3$, 400 MHz for ^{1}H and 100 MHz for ^{13}C NMR. Coupling constants (J) are in Hz.

signs of iodation, probably because the addition of iodine was quickly followed by elemination.[17] Both products were previously reported and their identity was confirmed by comparing their spectral data with the literature.[18,19]

Mechanistic Considerations. The relative stereochemistry of **5** was based on the ROESY/NOESY data, modeling data, and comparison of ^{13}C NMR data and J values with those of related compounds.[15,16] A modeling study suggested the β orientation of H-7. The opposite orientation of both oxygen functionalities is chemically and mechanistically expected, as it is known that hydration of oxiranes occurs by a trans periplanar ring opening by an incoming nucleophile (water) upon the more substituted C atom of the epoxide ring, while simultaneously, the epoxide oxygen is complexed by a protic or Lewis acid.[17] In these cases, a mercuronium ion is expected to form, exposing the epoxide oxygen to a carbocationic center only five or six atoms removed. As the mercuronium ion attracts a lone pair of electrons on the epoxide oxygen atom, ring opening of both mercuronium ion and epoxide occurs in a concerted fashion, while a water molecule approaches the carbocation being formed by the epoxide opening at C-8. Simultaneously, this partial charge attracts water and then undergoes hydration by the water molecule by a trans periplanar arrangement of atoms. Molecular modeling of the conversion of **4** to **5** (Figure 1) is illustrative of how **5** is formed, and the same rationale can be applied to explain the formation of the other oxymercuration−demercuration product **6**, in which the C-7/C-8 epoxide O attacks the alternate mercuronium ion formed at $\Delta^{11,12}$ via a six-membered intramolecular ring forming reaction.

This is also the case for intermediates leading to products **7** and **8** yielding a cis 2,6 and a trans 2,6 pyran ring, respectively. A transannular olefinic site in **6** can later undergo an additional, non-ring-forming hydridomercuration−demercuration by attack of borohydride rather than solvent on the incipient mercuronium ion. Why this is preferred over hydration is a matter of speculation at this point, but may simply be due to an excessive amount of borohydride and mercuric acetate used in the reaction.

For the products **9** and **10**, a bromonium ion forms at the $\Delta^{11,12}$ position, but in this case the bromonium ion is attacked by the epoxide at the more substituted C-12 position, giving a bromohydrin-like ring opening and again favoring the trans periplanar orientation of orbitals about the epoxide during ring opening and hydration. Both bromides gave seven-membered rings as opposed to **6**−**8**, which gave six-membered rings. Clearly, the mercuronium ion gives anti-Markovnikov- and Markovnikov-oriented products. For example, **5** undergoes a C-4/C-7 Markovnikov cyclization as well as a C-11/C-12 Markovnikov hydration. On the other hand, **6** undergoes an anti-Markovnikov cyclization between C-7/C-11 and a C-3/C-4 Markovnikov hydration. For **7** and **8**, the 3,4 double bond is unreacted, but cyclizations are anti-Markovnikov. For **7**, the bridgehead protons are syn to one another, while in **8** they are anti. In **5**, the cyclization is an allowed 5-exo-tet, while for **6**−**8**, an allowed 6-exo-tet occurs. Likewise, hypobromination giving **9** and **10** occurs via a bromonium ion ring opening to furnish Markovnikov-oriented seven-membered ring products by an allowed 7-exo-tet cyclization. The five-membered Markovnikov ring in **5** is formed because the transition state was stereoelectronically more favorable due to a facile ring flip of the epoxide of **4** so that the oxygen atom was oriented below the 3,4 mercuronium ion and could therefore select the more desirable tertiary carbonium ion. In the formation of **6**−**8** the mercuronium ion forms across the 11,12 double bond, so that the more substituted side of the double bond (C-12) would have provided a seven-membered ring that was less accessible due to torsional strain and was not thermodynamically preferred over a six-membered ring. Presumably, inherent transannular transition state strain and a thermodynamic preference for six- over seven-membered rings thus switched these cyclizations from Markovnikov to anti-Markovnikov orientations. In **7** and **8**, the ring fusions were respectively syn and anti, which is purely a reflection of the starting geometry of the olefin before approach of the Hg(II) species (methyl up or methyl down). Finally, the isolated hydrations that occurred for **5** and **6**, presumably after ring closure, across the $\Delta^{11,12}$ and $\Delta^{3,4}$, respectively, were oriented Markovnikov. The expected product regiochemistry was readily accommodated by flexibility in these portions of the (still) macrocyclic ring systems, and more importantly, a ring closure was not also involved in the reaction exerting an overriding stereoelectronic control of the issue of Markovnikov versus anti-Markovnikov addition.

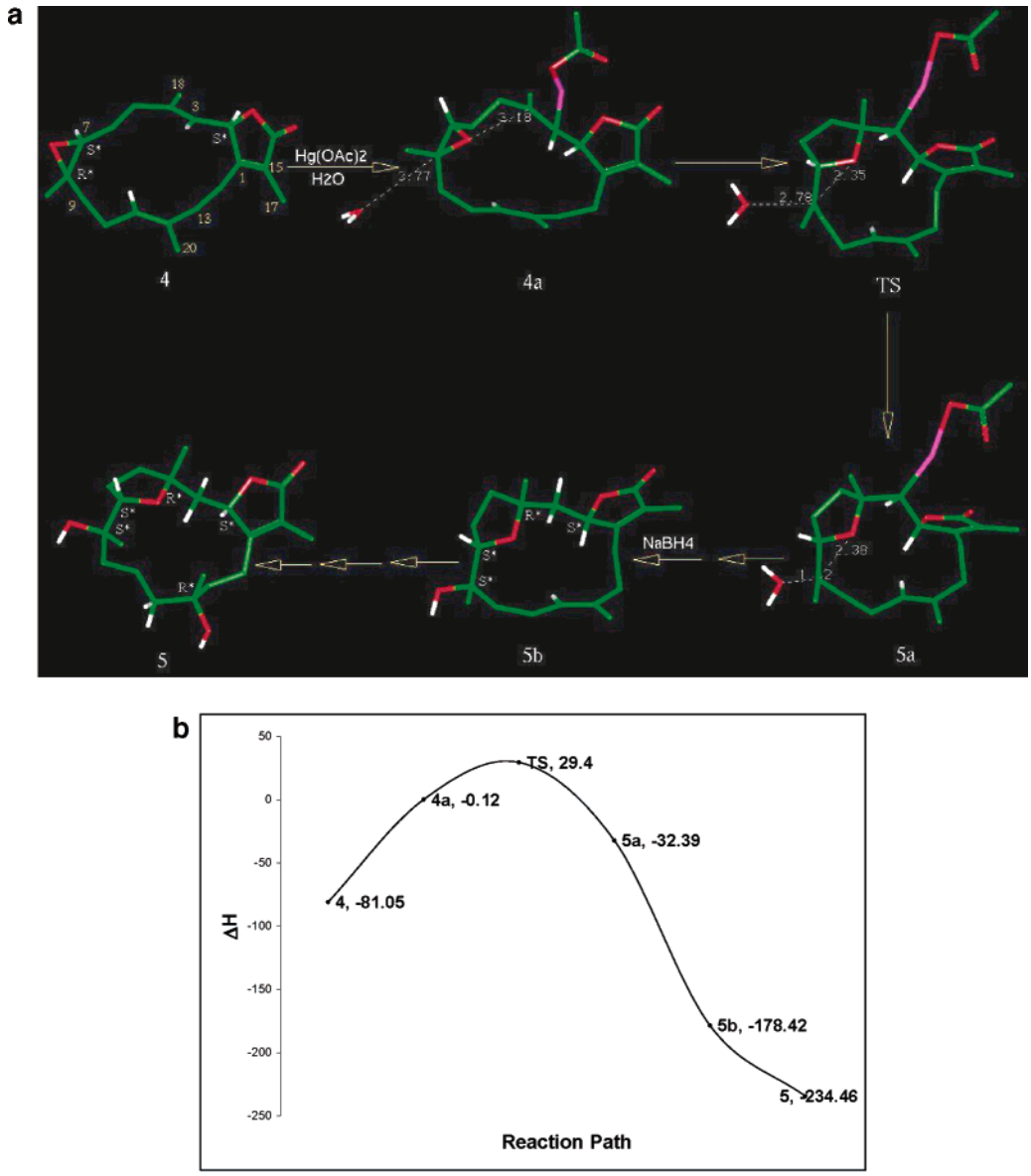

Figure 1. Structures and energies of proposed intermediates and transition state (TS) involved in conversion of **4** to **5**. (a) Reaction path showing important structures. Atoms are colored as follows: C, green; O, red; Hg, magenta; H, white. Only important hydrogens are shown for clarity. (b) Plot of ΔH_f of structures shown in (a).

Calculation of the Transition State Leading to 5. The transition state to **5** was calculated in order to predict relative stereochemistry of the products. Since most reactions are expected to proceed in a similar fashion, conversion of **4** to **5** was studied in detail, and the results were utilized to predict the stereochemistry for other products. The proposed reaction path based on a concerted mechanism, as suggested by computational studies, is presented in Figure 1. Structures **4a**, **5a**, and **5b** appeared as stable intermediates or stationary points on the reaction path, as confirmed by the frequency calculations. The structure of the TS was verified as a "true" TS by the presence of one and only one imaginary (negative) frequency.

As explained before, the electrophilic attack of mercury(II) as $^{+}$Hg(OAc) on the C-3/C-4 double bond of compound **4**, as per the Markovnikov addition, results in formation of intermediate **4a**. This appears to be followed by several processes simultaneously: attack of a water molecule on C-8 causing the epoxide ring to open and intramolecular attack of the resultant negatively charged oxygen on C-4 to give the TS (Figure 1). As it is clearly seen, in the TS the water molecule is weakly bonded to C-8 (2.78 Å) while the furan ring is almost completely formed. Thus, the TS appears to be a "product-like" transition state. In the next stationary point, **5a**, the bond between the water molecule and C-8 seems to be completely formed (1.62 Å) and the tetrahydrofuran oxygen appears to move further away from C-8 (2.38 Å). Reaction with one more molecule of water (not shown) and $NaBH_4$ would then result in formation of intermediate **5b**. The first phase of the reaction involving the C-3/C-4 double bond and the epoxide ring can be considered to be complete at this stage. The reaction path clearly suggests the relative stereochemistry at C-4, C-7, and C-8 to be *R**, *S**, and *S**, respectively (Figure 1). The subsequent reactions involving the C-11/C-12 double bond would finally give the product, **5**, which was isolated and characterized. The relative stereochemistry for C-12 in **5** was then proposed based on MD simulations as described later. The heats of formation (ΔH_f) for the intermediates and the TS are shown in Figure 1b. The energetic profiles of the intermediates and the TS clearly support the proposed reaction path.

Since the reaction most likely involves a concerted transition state (TS) and several variables (bond-making

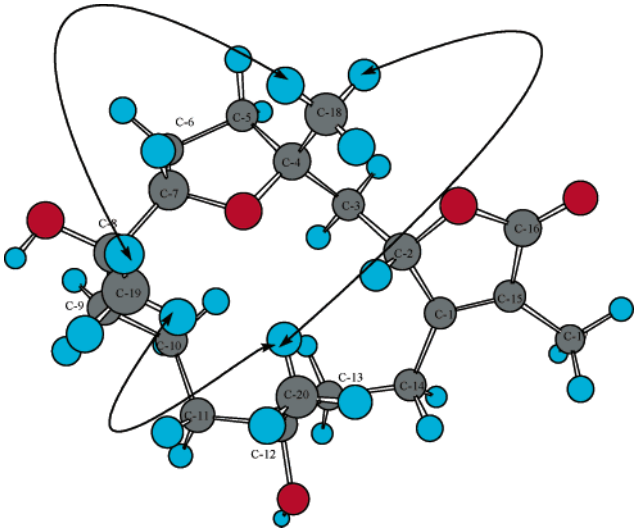

Figure 2. Lowest energy conformation of **5** is shown as a Chem 3D file, but calculated by molecular dynamics and simulated annealing in Sybyl v6.5 (Tripos Associates). Arrows indicate key ROESY correlations.

and -breaking processes), it is rather challenging to accurately model and identify all the intermediates and the TS. Thus, the reaction may involve more intermediates/stationary points than suggested by the current calculations. For the same reasons, the TS could not be optimized beyond a GNORM of 0.1. However, on the basis of the frequency calculations, it appears to be a realistic TS for the reaction. Also, we strongly feel that the calculated reaction path is reasonable enough to correctly predict the relative stereochemistry of the product, which was the sole purpose of the study.

Assignment of Relative Stereochemistry. The lowest energy conformer obtained by the MD simulations for every possible isomer of each of the compounds was analyzed with respect to their ability to explain the experimentally obtained NOESY/ROESY correlations. In addition to mechanistic feasibility, as described above for **5**, MD was also considered in order to propose relative stereochemistry of the compounds. Thus, analysis of the lowest energy conformer and mechanistic considerations for **5** enabled us to assign C-7/C-8 relative stereochemistry as *S**,*S**. The lowest energy conformer could also explain the ROESY correlations between all the methyl groups as representated in Figure 2. These ROESY correlations also established the relative stereochemistry at C-4 and C-12 as *R**. Comparing the ^{13}C chemical shift values and the coupling data of C-7 in **5** and **6**, H-7 can be assigned as β-oriented. Also on the basis of the same argument as above and the strong ROESY correlations between H_3-18, H_3-19, and H_3-20, all these methyl groups can be assigned to be α-oriented and hence establish the relative stereochemistry of the chiral centers C-4 and C-12 as *S** and *R**, respectively. For **7**, the β orientation of H-12 was indicated from its NOESY correlation with the β-oriented H-2. H-12 showed NOESY correlation with H-11, which in turn shows NOESY correlation with H-7, suggesting the β orientation of H-7 and H-11. These NOESY correlations once again are well supported by the lowest energy conformer for **7** and helped to assign all the stereocenters, namely, C-7, C-8, C-11, and C-12, as *S**. As discussed earlier, **8** is an epimer of **7** at C-11 on the basis of the NMR data. Applying the same argument as **6** to compound **9**, H_3-19 can be assigned to be α-oriented and the ROESY correlation between H_3-19 methyl with H_3-20 indicated *S** and *R** relative stereochemistry at C-8 and C-11, respectively. The same lowest

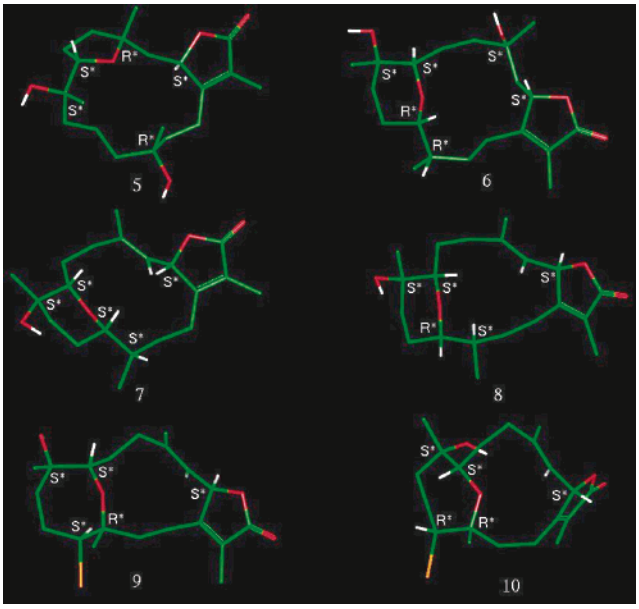

Figure 3. Relative stereochemistry of **5**−**10** based on MD simulation, reaction mechanism, and NOESY/ROESY correlations. The atoms are colored in a similar fashion as in Figure 1. Only important hydrogens are shown for clarity.

energy conformer that complied with the ROESY correlations suggested C-11 to have the relative stereochemistry *S**. Comparing the NMR data for **10** has confirmed that the **9** and **10** are epimers at position C-11. Thus, the relative stereochemistry for **5**−**10** was assigned considering the NOESY/ROESY correlations, lowest energy conformers, and mechanistic possibilities and are represented in Figure 3. Although the crystal structure of sarcophine has been known since 1974, it was not until recently that the absolute stereochemistry of this compound was established using CD measurements.[6,20] König and co-workers recently assigned the absolute stereochemistry of sarcophine as 2*S*, 7*S*, 8*S*.[20] This was based on CD data of sarcophine and applying Mosher's method on the related cembranoid sarcoglaucol-16-one.[20] This was identical and further supports our assignment of the stereochemistry of analogues **5**−**10** based on NOESY/ROESY data and molecular modeling.

Antiproliferative Activity. The antiproliferative effects of sarcophine and sarcophine-derived compounds on malignant +SA mammary epithelial cell growth after 4 days in culture are shown in Figure 4. Treatment with 0−10 μM of sarcophine had no effect, whereas treatment with 100−1000 μM sarcophine caused a dose-responsive decrease in +SA cell growth, as compared to controls (Figure 4). Similarly, treatment with 100 μM **12** (Figure 4) and 1−100 μM **10** (Figure 4) was found to inhibit +SA cell growth. Similar studies showed that treatment with up to 100 μM **5**−**9** and **11** had no effect on the growth of malignant +SA mammary epithelial cells as compared to controls. These studies demonstrate that treatment with 100−1000 μM sarcophine induced a large reduction in malignant +SA mammary epithelial cell proliferation in vitro. However, only a few of the sarcophine semisynthetic derivatives produced were found to display antiproliferative activity on mammary cancer cells, and these effects were not found to be more potent than the native compound. Additional studies are required to determine the antiproliferative effects of these compounds on other types of cancer cells.

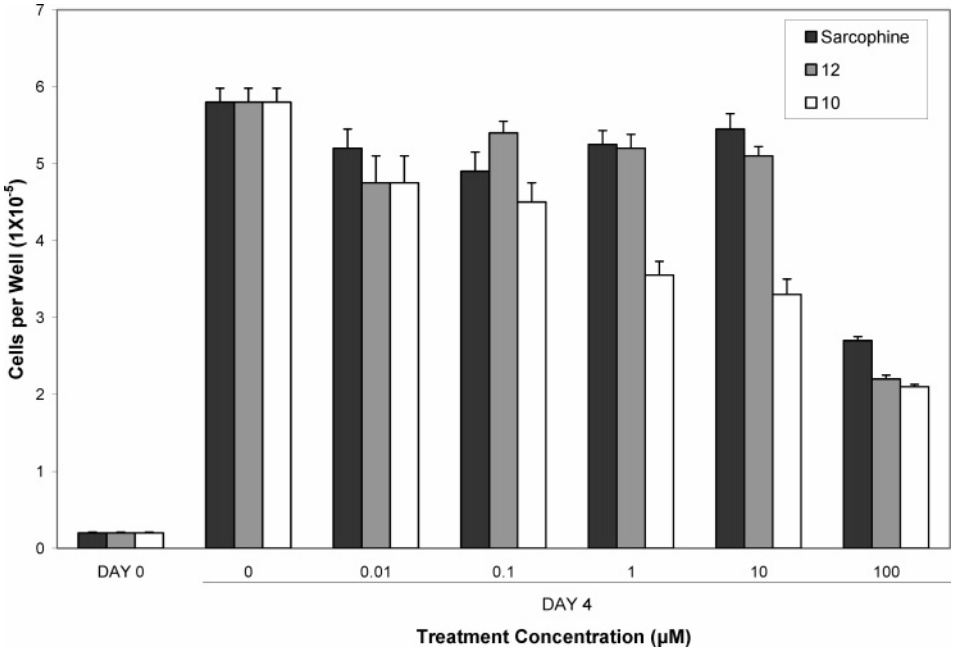

Figure 4. Effects of various doses of sarcophine and sarcophine-derivatives **12** and **10** on malignant (+SA) mammary epithelial cell proliferation in culture. Data points indicate the mean cell count/well + SEM for 6 replicates in each treatment group after 4 days in culture.

Conclusion

Six new hydroxylated and brominated semisynthetic derivatives of sarcophine (**5**−**10**) are reported. The stereochemistry of these analogues was established using NOESY/ROESY data and molecular modeling. The antiproliferative activity of **5**−**10** in comparison to the parent compound is reported. Since hydroxylated derivatives are known to improve the anticancer activity, the loss of activity in compounds **5**−**8** clearly suggests the importance of more than one macrocyclic double bond for anticancer activity.

Experimental Section

General Experimental Procedures. Melting points are uncorrected. The ^{1}H and ^{13}C NMR spectra were recorded in $CDCl_3$, on a NMR spectrometer operating at 400 MHz for proton and 100 MHz for carbon. The HRFABMS experiments were conducted at the University of Kansas. The HRFTMS experiment was conducted at the University of Mississippi using FTMS with electrospray ionization. TLC analyses were carried out on precoated silica gel G_{254} 500 μm, using the developing systems hexanes−EtOAc (70:30) and CH_3CN−$CHCl_3$ (40:60). For preparative TLC Si gel 60 PF 254 was used. For reversed-phase column chromatography prepacked disposable C-18 Si gel solid-phase extraction columns (1 g each) were used. For column chromatography, Si gel 70−230 mesh was used.

Materials. The soft coral *Sarcophyton glaucum* was collected by scuba from sand bottoms at −5 m at Hurghada, on the Egyptian Red Sea coast, in June 2003. A voucher specimen (03RS24) is deposited in the Department of Basic Pharmaceutical Sciences, School of Pharmacy, University of Louisiana at Monroe, LA. The wet frozen soft coral (680 g) was coarsely minced and percolated with 2-propanol at room temperature (1 L × 4). The extract (86 g) was then concentrated under vacuum and chromatographed on silica gel using hexanes−EtOAc (4:1) to yield a fraction rich in sarcophine, which was further recrystallized from EtOAc to afford 1.5 g of sarcophine (**4**). The identification of **4** was accomplished by comparing its physical and spectral data with the previously reported data.[6]

Computational Studies. Computational studies were performed on a Silicon Graphics Octane 2 workstation, equipped with two parallel R12000 processors, V6 graphics board and 512 MB memory. Energy minimizations and molecular dynamics were accomplished in the Discover module of InsightII 2000 (Accelrys Inc., San Diego, CA). Semiempirical calculations were performed using MOPAC 6.0 interfaced with InsightII 2000.

Calculation of Transition State. Structures of **4**, important intermediates, and **5** were submitted for minimization by the semiempirical AM1 method. AM1 optimizations were run with EF algorithm to a GNORM of 0.01 for the ground states and 0.1 for the transition state using the PRECISE option. The approximate structure for the transition state was first obtained using the SADDLE protocol followed by optimization as described above. Minimizations were carried out without any conformational or symmetry restrictions. All stationary points were characterized vigorously by computing vibrational frequencies with the FORCE option. Ground states and stable intermediates were confirmed by the absence of any imaginary (negative) frequency, while the transition state was identified by the presence of only one vibration with an imaginary frequency.

Molecular Dynamics (MD) Simulations. All possible isomers of **5**−**10** were subjected to molecular dynamics calculation using simulated annealing protocol as follows. The structures were first minimized using 1000 steps of conjugate gradients to remove any strain. This was followed by "heating" the structures to 800 K in steps of 100 K and equilibration for 15 ps at this temperature. Dynamics was then continued for a further 100 ps and the trajectory sampled every 1 ps to give a set of 100 conformers. Each conformer was then "cooled" to 300 K in steps of 100 K by a short MD run of 5 ps at each temperature. Finally, the structures were minimized to a gradient of 0.001 kcal mol^{-1} Å^{-1}. On the basis of this exhaustive search as well as mechanistic feasibility and important NOESY/ROESY correlations, possible isomers have been selected for each of **5**−**10**.

Antiproliferative Assay. The antiproliferative effects of sarcophine and sarcophine-derived compounds were tested in culture on the highly malignant +SA mouse mammary epithelial cell line maintained on serum-free media and containing 10 ng/mL EGF and 10 μg/mL insulin as mitogens, as described previously in detail.[21] Cells were plated at a density of 5 × 10^4 cells/well (6 wells/group) in 24-well culture plates and fed media containing various concentrations (0.01−1000 μM) of each compound. After a 4-day culture period, viable +SA cell number was determined by the 3-(4,5-dimethylthi-

azol-2yl)-2,5-diphenyl tetrazolium bromide (MTT) colorimetric assay as described previously.[21]

Reaction of Mercuric Acetate and Sodium Borohydride with 4. About 55 mg of **4** was dissolved in 5 mL of 20% aqueous acetone. To this solution was added 1 g of $Hg(OAc)_2$, and the mixture was stirred for 1 h at room temperature. About 500 mg of $NaBH_4$ was gradually added, and the reaction mixture was stirred for 5 min. The reaction was stopped by adding cold water, and the reaction mixture was extracted with $CHCl_3$ (2 × 10 mL). The $CHCl_3$ layer was evaporated under vacuum to give a crude product mixture (40 mg). The residue was fractionated on silica gel 60 (<63 μm particle size, 30 g) using isocratic elution with hexane−EtOAc (50:50) followed by CH_3CN−$CHCl_3$ (10:90) to give a mixture of **5**, **6** and a mixture of **7**, **8** in separate fractions. The later mixture was further chromatographed on silica gel (2 g) using EtOAc−$CHCl_3$−NH_4OH gradient elution to yield **7** (5.6 mg, R_f 0.32, hexane−EtOAc, 70:30) and **8** (7.3 mg, R_f 0.21, hexane−EtOAc, 70:30). The former fraction was further chromatographed by silica gel preparative TLC using $CHCl_3$−CH_3CN (90:10) to afford **5** (7.5 mg, R_f 0.62, $CHCl_3$−CH_3CN, 60:40) and **6** (11.4 mg, R_f 0.36, $CHCl_3$−CH_3CN, 60:40).

Reaction of *N*-Bromosuccinimide with 4. A solution of 50 mg of NBS in 2 mL of 20% aqueous acetone was slowly added to 2 mL of solution of **4** (50 mg) in 20% aqueous acetone. The reaction mixture was stirred for 5 min at room temperature and worked up as in the previous reaction. The residue (67 mg) was chromatographed by MPLC on a C-18 reversed-phase silica gel prepacked cartridge (2 g) using CH_3CN−H_2O, gradient elution, to afford **9** (6.9 mg, R_f 0.14, hexane−EtOAc, 70:30) and **10** (4.1 mg, R_f 0.20, hexane−EtOAc, 70:30).

Reaction of Iodine and Triphenyl Phosphine with 4. A solution of 50 mg of Ph_3P in 2 mL of CH_2Cl_2 was added dropwise to a solution containing 55 mg of **4** in 1 mL of CH_2Cl_2 maintained in an ice bath. To this reaction mixture was gradually added a solution of 50 mg of I_2 in 2 mL of CH_2Cl_2. The reaction mixture was stirred in an ice bath for 6 h and worked up as in the previous reactions. The residue (85 mg) was chromatographed on silica gel using hexane−$CHCl_3$, gradient elution, to afford two known compounds, iso-sarcophinone (**11**) (15.4 mg, R_f 0.71, hexane−EtOAc, 70:30) and (+)-sarcophytoxin B (**12**) (19.2 mg, R_f 0.53, hexane−EtOAc, 70:30).[15,16]

Compound 5: colorless oil, $[\alpha]_D^{25}$ −8.8° (*c* 0.57, $CHCl_3$); UV λ_{max} (log ϵ) ($CHCl_3$) 274 (2.24), 239 (3.15) nm; IR ν_{max} (neat) 3425, 2983−2840, 1752, 1681, 1488, 1366, 1183, 766 cm^{-1}; ^1H and ^{13}C NMR, see Table 1; HRFABMS *m/z* 353.2328 $(M + H)^+$ (calcd for $C_{20}H_{33}O_5$, 353.2328).

Compound 6: colorless oil, $[\alpha]_D^{25}$ 11.6° (*c* 0.43, $CHCl_3$); UV λ_{max} (log ϵ) (MeOH) 261 (3.31), 246 (3.35), 241 (3.36), 226 (3.30) nm; IR ν_{max} (neat) 3351, 2932−2850, 1742, 1679, 1477, 1366, 1210, 766 cm^{-1}; ^1H and ^{13}C NMR, see Table 2; HRFABMS *m/z* 353.2349 $(M + H)^+$ (calcd for $C_{20}H_{33}O_5$, 353.2328).

Compound 7: colorless oil, $[\alpha]_D^{25}$ +43.9° (*c* 0.11, $CHCl_3$); UV λ_{max} (log ϵ) ($CHCl_3$) 271 (3.13), 239 (3.35) nm; IR ν_{max} (neat) 3440, 2924−2852, 1736, 1673, 1462, 1386, 1285, 776 cm^{-1}; ^1H and ^{13}C NMR, see Table 1; HRFABMS *m/z* 335.2232 $(M + H)^+$ (calcd for $C_{20}H_{31}O_4$, 335.2222).

Compound 8: colorless oil, $[\alpha]_D^{25}$ +35.7° (*c* 0.14, $CHCl_3$); UV λ_{max} (log ϵ) ($CHCl_3$) 277 (2.77), 239 (3.02) nm; IR ν_{max} (neat) 3430, 2932−2861, 1752, 1681, 1467, 1366, 1233, 766 cm^{-1}; ^1H and ^{13}C NMR, see Table 2; HRFABMS *m/z* 335.2213 $(M + H)^+$ (calcd for $C_{20}H_{31}O_4$, 335.2222).

Compound 9: colorless oil, $[\alpha]_D^{25}$ +68.2° (*c* 0.10, $CHCl_3$); UV λ_{max} (log ϵ) ($CHCl_3$) 277 (2.16), 224 (2.73) nm; IR ν_{max} (neat) 3450, 2980−2850, 1761, 1466, 1390, 1257, 1028, 766 cm^{-1}; ^1H and ^{13}C NMR, see Table 2; HRFABMS *m/z* 413.1319 $(M + H)^+$ (calcd for $C_{20}H_{29}BrO_4$, 413.1327).

Compound 10: colorless oil, $[\alpha]_D^{25}$ +11.9° (*c* 0.10, $CHCl_3$); UV λ_{max} (log ϵ) ($CHCl_3$) 280 (2.57), 239 (3.19) nm; IR ν_{max} (neat) 3457, 2990−2866, 1761, 1467, 1386, 1231, 1040, 766 cm^{-1}; ^1H and ^{13}C NMR, see Table 2; HRFTMS *m/z* 435.1143 $(M + Na)^+$ (calcd for $C_{20}H_{29}BrO_4$, 435.1146).

Acknowledgment. A. M. Crider and R. A. Hill, University of Louisiana at Monroe, are acknowledged for their valuable suggestions and help. T. Williams, Mass Spectrometry Laboratory, University of Kansas, and D. C. Dunbar, National Center for Natural Products Research, University of Mississippi, are acknowledged for MS analyses.

Supporting Information Available: ^1H, ^{13}C, HMQC, and HMBC NMR spectra of compounds **5**−**10** are available free of charge via the Internet at http://pubs.acs.org.

References and Notes

(1) Lippman, S. M.; Spitz, M. R. *J. Clin. Oncol*. **2001**, *19* (suppl 18), 74s−82s.
(2) Valagussa, P.; Bonadonna, G. *Cancer Chemother. Biol. Response Modifiers* **2002**, *20*, 493−517.
(3) Wahlberg, I.; Eklund, A. M. *Prog. Chem. Org. Nat*. **1992**, *59*, 141−294.
(4) Blackman, A. J.; Bowden, B. F.; Coll, J. C.; Frick, B.; Mahendran, M.; Mitchell, S. J. *Aust. J. Chem.* **1982**, *35*, 1873−1880.
(5) Kobayashi, M.; Nakagawa, T.; Mitsuhashi, H. *Chem. Pharm. Bull.* **1979**, *27*, 2382−2387.
(6) Bernstein, J.; Shmeuli, U.; Zadock, E.; Kashman, Y.; Ne'eman, I. *Tetrahedron* **1974**, *30*, 2817−2824.
(7) Ne'eman, I.; Fishelson, L.; Kashman, Y. *Toxicon* **1974**, *12*, 593−598.
(8) Erman, A.; Ne'eman, I. *Toxicon* **1977**, *15*, 207−215.
(9) Suleimenova, A. M.; Kuznetsova, T. A.; Denisenko, V. A.; Gorshkova, I. A.; Elyakov, G. B. *Khim. Prir. Soedin*. **1990**, *6*, 762−765.
(10) El Sayed, K. A.; Hamann, M. T.; Waddling, C. A.; Jensen, C.; Lee, S. K.; Dunstan, C. A.; Pezzuto, J. M. *J. Org. Chem*. **1998**, *63*, 7449−7455.
(11) Katsuyama, I.; Fahmy, H.; Zjawiony, J. K.; Khalifa, S. I.; Kilada, R. W.; Konoshima, T.; Takasaki, M.; Tokuda, H. *J. Nat. Prod*. **2002**, *65*, 1809−1814.
(12) Tsankova, E.; Enev, V.; Simova, S. *Tetrahedron* **1984**, *40*, 2435−2440.
(13) Bernardelli, P.; Moradei, O. M.; Friedrich, D.; Yang, J.; Gallou, F.; Dyck, B. P.; Doskotch, R. W.; Lange, T.; Paquette, L. A. *J. Am. Chem. Soc.* **2001**, *123*, 9021−9032.
(14) Rodriguez, A. D.; Pina, I. C.; Acosta, A. L.; Barnes, C. L. *Tetrahedron* **2001**, *57*, 93−107.
(15) Rodriguez, A. D.; Pina, I. C.; Acosta, A. L.; Ramirez, C.; Soto, J. J. *J. Org. Chem.* **2001**, *66*, 648−65.
(16) El Sayed, K. A.; Orabi, K. Y.; Dunbar, D. C.; Hamann, M. T.; Avery, M. A.; Sabnis, Y. A.; Mossa, J. S.; El-Feraly, F. S. *Tetrahedron* **2002**, *58*, 3699−3708.
(17) Sykes, P. *A Guide Book to Mechanism in Organic Chemistry*, 6th ed.; Orient Longman Limited: Hyderabad, India, 2000; p 190.
(18) Czarkie, D.; Carmely, S.; Groweiss, A.; Kashman, Y. *Tetrahedron* **1985**, *41*, 1049−1056.
(19) Kobayashi, M.; Hirase, T. *Chem. Pharm. Bull.* **1990**, *38*, 2442−2445.
(20) Gross, H.; Wright, A. D.; Beil, W.; König, G. M. *Org. Biomol. Chem.* **2004**, *2*, 1133−1138.
(21) McIntyre, B. S.; Briski, K. P.; Gapor, A.; Sylvester, P. W. *PSEBM* **2000**, *224*, 292−301.

NP0497393